

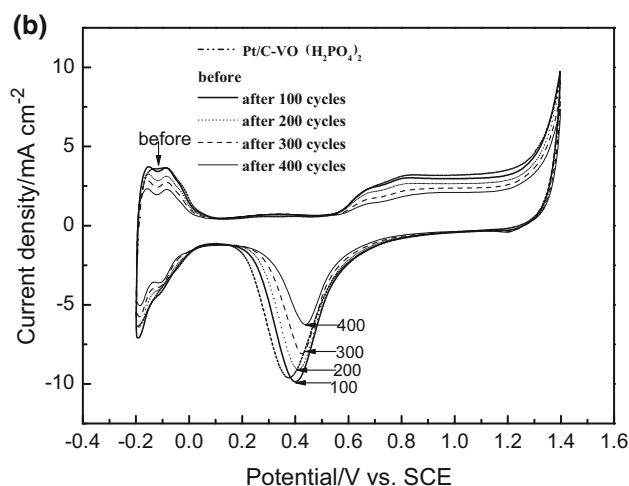
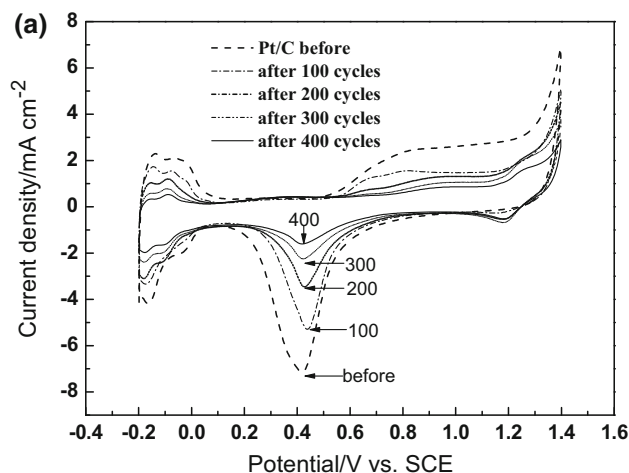
Improving the durability of Pt/C catalyst in PEM fuel cell by doping vanadium phosphate oxygen

Yang Li¹ · Hongfeng Xu¹ · Hong Zhao¹ · Lu Lu¹ · Xin Sun¹

Received: 19 June 2015 / Accepted: 26 October 2015 / Published online: 7 November 2015
© Springer Science+Business Media Dordrecht 2015

Abstract This study investigated the addition of vanadium phosphate [VO(H₂PO₄)₂] to platinum/carbon (Pt/C) to prepare Pt/C–VO(H₂PO₄)₂ catalyst. Pt/C electrocatalyst was treated with vanadium pentoxide (V₂O₅) and phosphoric acid concentration to produce VO(H₂PO₄)₂. This combination improved the durability of proton exchange membrane fuel cells (PEMFCs); nonetheless, the addition of VO(H₂PO₄)₂ did not negatively affect the homogenization and electrochemical activity of the Pt/C catalyst. Moreover, the presence of VO(H₂PO₄)₂ was confirmed by the X-ray diffraction pattern and the energy spectrum. The ideal VO(H₂PO₄)₂ ratio (6 %) was determined, and the VO(H₂PO₄)₂ was imported to reduce oxidation in the weak acid environment of the PEMFCs cathode catalyst. When the fuel cell operates at high potential, VO²⁺ is oxidized to VO₂⁺. This preferential oxidation protects carbon carriers against oxidation. When the fuel cell returns to normal working potential, the VO₂⁺ is restored to VO²⁺. VO²⁺ is a reserve for the protection of carbon carriers at the subsequent instance of high potential. The oxide between the Pt particles coated the surface of the carbon carriers, thus limiting the aggregation and loss of Pt. These two functions enhance the durability of fuel cell electrodes.

Graphical Abstract



✉ Hongfeng Xu
hfxu@fuelcell.com.cn

Yang Li
l_i_yang_happy@126.com

¹ Liaoning Province Key Laboratory for New Energy Battery,
Dalian Jiaotong University, 794 Huanghe Road,
Dalian 116028, China

Keywords VO(H₂PO₄)₂ · Proton exchange membrane fuel cell · Pt/C catalyst · Hydrothermal method · Redox reaction

1 Introduction

With the increasing consumption of nonrenewable energy (oil and coal) sources and with pressing air pollution problems, new clean energy sources need to be developed and promoted urgently. A fuel cell is an electrochemical device that directly converts chemical energy into electrical energy. Reactions occur continuously as long as fuels and oxidants are supplied to the electrodes and remain connected. Among the various types of fuel cells, proton exchange membrane fuel cells (PEMFCs) are promising because they are environmentally friendly and have several advantages over conventional energy-converting devices, including high efficiency and power density. Thus, PEMFCs are unique across a wide range of portable, stationary, and transportation power applications. Hydrogen is the most commonly used fuel, and it is usually accompanied by oxygen as the typical oxidant. PEMFCs contain Pt/C as a cathode electrocatalyst. Moreover, these cells typically possess carbon-supported, nanosized Pt and Pt alloy catalysts for both anodes and cathodes. Thus far, carbon materials are most widely studied as catalyst supports for PEMFCs because of their high electrical conductivity, large surface area, and well-developed pore structures. Such materials include carbon black, carbon nanofibers, carbon nanotubes, and carbon nanohorns. Nonetheless, the corrosion of the catalysts in PEMFCs is a significant hindrance to their commercialization in stationary and transportation power applications. Previous studies have indicated that the performance and durability of PEMFCs gradually decline because of the deterioration in the performance of their catalysts. In addition, such PEMFCs operate for thousands of hours or under special conditions. The corrosion of carbon support in the catalysts is a main factor affecting catalyst performance [1]. Other factors that deteriorate the performance of catalysts are Pt particle agglomeration and particle growth [2–5], Pt loss and redistribution [6–9], and the poisonous effects of contaminants [10–12].

Tremendous efforts have been exerted to improve catalyst stability. Numerous investigations have confirmed that the catalytic activity in Pt–M binary and ternary alloys is considerably higher than that in Pt catalysts for oxygen reduction reaction (ORR). The elements that are most suitable for alloying with Pt are determined from among a variety of transition metals. For example, ORR kinetics reflect a threefold to fivefold improvement when Pt is alloyed with Co, Ni, and Cr as compared with the scenario involving Pt catalysts [13–15]. Nonetheless, the size, shape, and composition of particles also significantly influence the activity of Pt–M alloy catalysts, along with the method of preparing alloy nanoparticles [16]. Ordinary carbon materials, such as graphite fiber and graphene, have

also been graphitized further to improve catalyst performance. However, improved corrosion resistance cannot compensate for the disadvantage in terms of high-specific surface area and high conductivity; thus, surface area, conductivity, corrosion resistance, and price must be balanced to generate good fuel cell catalysts. Given these problems, the introduction of the concept of sacrificial anode protection into the cathode of PEMFCs is promising in the field of electrochemical corrosion. Vanadium phosphate $[\text{VO}(\text{H}_2\text{PO}_4)_2]$ is added to the original Pt/C catalyst to prepare Pt/C–VO(H₂PO₄)₂. This combination improves the performance and reliability of catalysts. The common valences of vanadium are V, VI, III, and II, and numerous compounds belonging to almost all classes are synthesized under hydrothermal conditions. When a fuel cell operates at high potential, VO²⁺ is oxidized to VO₂⁺. This preferential oxidation protects the carbon support carriers against oxidation. When the fuel cell returns to normal working potential, VO₂⁺ is restored to VO²⁺. VO²⁺ is a reserve for the protection of carbon carriers at the subsequent instance of high potential.

2 Experimental

2.1 Materials and chemicals

The following chemicals were used in the current study: V₂O₅ (≥99.0 %) supplied by Tianjin Guangfu Fine Chemical Factory, H₃PO₄ (98 wt%) obtained from Tianjin Kermel Chemical Reagent Co., Ltd., China, and Pt/C catalyst (Pt 50 %) purchased from Dalian Sunrise Power Co., Ltd. All chemicals were of analytical reagent grade and were utilized without further purification. All aqueous solutions were prepared using deionized water.

2.2 Modification of Pt/C–VO(H₂PO₄)₂ catalyst

The Pt/C–VO(H₂PO₄)₂ catalyst was prepared as follows: First, V₂O₅ was dissolved in deionized water (1000 mL). Second, H₃PO₄ and Pt/C were added sequentially to the aforementioned solution. The mixture was stirred until a homogeneous solution was obtained. The autoclave was sealed carefully and then heated at 180 °C for 16 h to facilitate a hydrothermal reaction. Once the reaction was completed, the autoclave was naturally cooled to room temperature. Finally, the Pt/C–VO(H₂PO₄)₂ catalyst obtained was washed thoroughly with deionized water and dried in air for further characterization. Pt/C catalysts with different ratio of VO(H₂PO₄)₂ were prepared. Pt/C were replaced by XC-72 and the test was repeated to prepare C–VO(H₂PO₄)₂ catalyst.

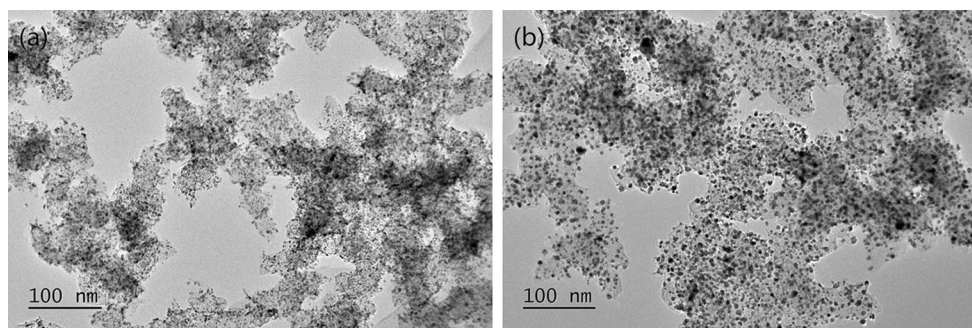


Fig. 1 TEM images of the **a** Pt/C and **b** Pt/C–VO(H₂PO₄)₂ catalyst

Furthermore, 5 mg of dried Pt/C–VO(H₂PO₄)₂ catalyst powder, 50 μ L of Nafion, and 2 mL of ethyl alcohol were mixed homogeneously for 90 min. A certain volume of the catalyst was placed on a glassy carbon (GC) electrode using a microsyringe given a Pt loading of 0.4 mg cm⁻².

2.3 Material characterization

The morphology of the Pt/C–VO(H₂PO₄)₂ catalyst was investigated by TEM measurements that were performed with a JEOL 2010 microscope operated at 200 kV.

The samples for transmission electron microscopy (TEM) were prepared by ultrasonically suspending the catalyst powder in ethanol and immersing a copper grid coated with carbon film. The X-ray diffraction (XRD) pattern of the Pt/C–VO(H₂PO₄)₂ catalyst was obtained using a powder X-ray diffractometer (PANalytical Empyrean) with Cu K α radiation.

2.4 Electrochemical measurements

Cyclic voltammetry (CV) and electrochemical impedance spectroscopy (EIS, 10 kHz–100 mHz) were performed at room temperature using a three-electrode cell. This cell was controlled at an Autolab electrochemical workstation (PGSTAT302 N, Ecochemie Co., the Netherlands) and consisted of the prepared GC electrode as the working electrode, an Hg/Hg₂Cl₂ electrode (SCE, saturated KCl, 0.214 V vs. NHE at 25 °C) as the reference electrode, and a Pt wire as the counter electrode. The background electrolyte was 0.5 M H₂SO₄. CV was conducted between –0.2 and 1.4 V (vs. SCE) at a scan rate of 50 mV s⁻¹. The electrochemically active surface area (ESA) was derived from the voltammetric profiles recorded at 50 mV s⁻¹ through integration with hydrogen under a potential deposition region. This area is calculated using Eq. (1):

$$ESA = \frac{Q_H}{Q_{ref}L_{Pt}}, \quad (1)$$

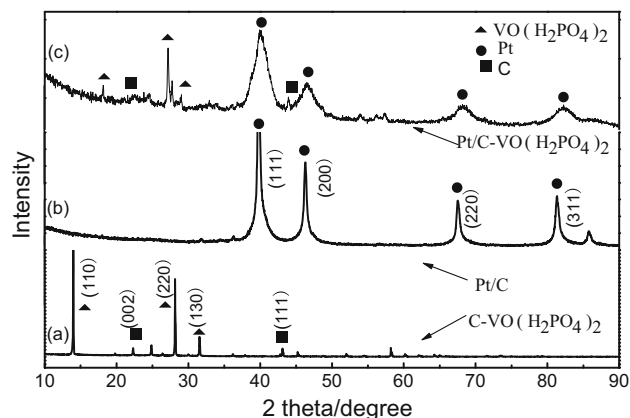


Fig. 2 XRD patterns of the **a** C–VO(H₂PO₄)₂, **b** Pt/C, **c** Pt/C–VO(H₂PO₄)₂ catalyst sample

where Q_H is the charge of hydrogen adsorption; Q_{ref} controls the monolayer adsorption of hydrogen on polycrystalline Pt [equal to 210 C (cm² Pt)⁻¹]; and L_{Pt} is the loading of Pt in the cathode [17].

2.5 Durability test

The durability test was conducted through repeated the CV test for 800 cycles at room temperature using a three-electrode cell. The ESA of Pt in the catalysts was computed using Eq. (1) to facilitate a comparison of the durabilities of Pt/C–VO(H₂PO₄)₂ and Pt/C catalyst.

2.6 Single-cell test

The membrane electrode assembly (MEA) was prepared by spraying of a mixed slurry of the catalysts and 5 wt% Nafion[®] ionomers dispersed in alcohol on the Nafion[®]-212 membranes (DuPont Co.). Pt loadings of 0.4 mg cm⁻² were maintained at both the anode and cathode. The effective electrode area was 10 cm².

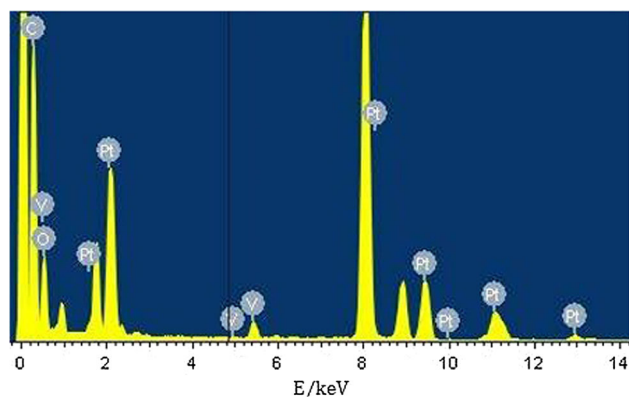


Fig. 3 EDS images of the Pt/C-VO(H₂PO₄)₂ catalyst

The PEMFCs performance of membrane electrode assembly (MEA) was tested through an in-house, single-fuel cell test setup. The stoichiometries of pure hydrogen and laboratory air were 1.1 and 2.5, respectively; these values represented the fuel and oxidant of the stoichiometric ratios. Moreover, the hydrogen and laboratory air were regulated by a mass flow controller (Brooks). Fuel cell performance was determined at 60 °C and a relative humidity of 80 % without back pressure.

3 Results and discussion

3.1 TEM and XRD analyses of the Pt/C-VO(H₂PO₄)₂ catalyst

Figure 1b presents the TEM image of the Pt/C-VO(H₂PO₄)₂ catalyst. This image indicates that the microstructures of the VO(H₂PO₄)₂ nanoparticles are characterized by uniformly distributed Pt nanoparticles on high-surface C. The Pt nanoparticles depicted in Fig. 1b are slightly larger than those shown in Fig. 1a. Nonetheless, the addition of VO(H₂PO₄)₂ did not impair the homogenization of the Pt/C catalyst.

Figure 2 displays the XRD patterns of (a) C-VO(H₂PO₄)₂, (b) Pt/C, (c) Pt/C-VO(H₂PO₄)₂ catalyst nanoparticles. The diffraction peaks in Fig. 2a located at 13.9°, 28.2°, and 31.56° are the characteristic peaks of VO(H₂PO₄)₂, corresponding to the diffraction by (110), (220), and (130) planes. The other diffraction peaks agree with the typical XRD patterns of VO(H₂PO₄)₂ (00-040-0038). A similar correspondence between Fig. 2b and Pt is also detected. The peaks at 39.9°, 46°, 67°, and 81° result from the diffraction by (111), (200), (220), and (311) planes. Another two peaks (26.3° and 44.1°) are designated as diffraction from (002) and (111) planes of C(00-001-0640). It is noticed that there is a little shift in intensity and the 2θ

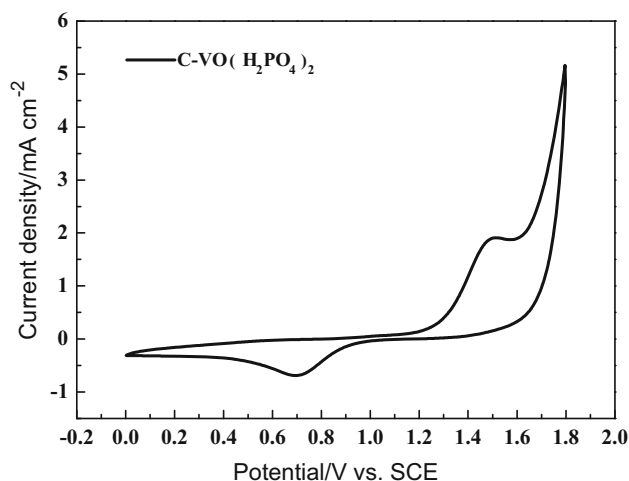


Fig. 4 CV curves of the C-VO(H₂PO₄)₂ catalyst at a scan rate of 50 mV/s in 0.5 M H₂SO₄ solution

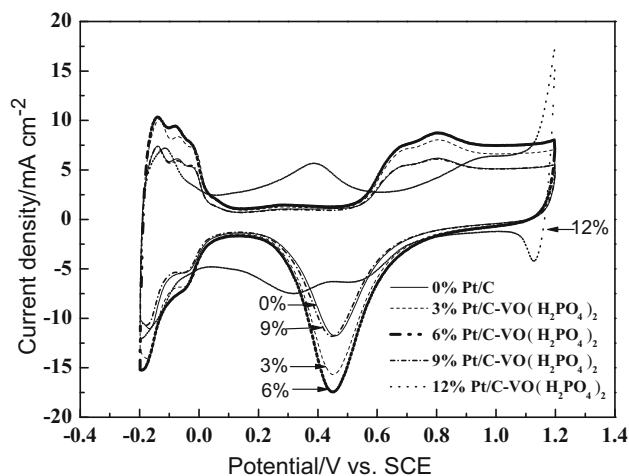


Fig. 5 CV curves of the different ratio VO(H₂PO₄)₂ doping in Pt/C catalyst at a scan rate of 50 mV/s in 0.5 M H₂SO₄ solution

of the diffraction peaks of VO(H₂PO₄)₂ in (c) compared with (b), which might be caused by the existence of Pt. Another fact which should be emphasized is that the peaks of VO(H₂PO₄)₂ in (c) are also the characteristic peaks of VO(H₂PO₄)₂ (00-021-1436). However, the addition of VO(H₂PO₄)₂ does not change the crystalline lattice of Pt. Therefore, the feature of Pt is still captured in the diffraction pattern.

Figure 3 presents the energy-dispersive spectroscopy (EDS) image of the Pt/C-VO(H₂PO₄)₂ catalyst. Moreover, the sample was dispersed on a copper substrate for TEM observation. The EDS spectrum in Fig. 3 suggests that the sample of the Pt/C-VO(H₂PO₄)₂ catalyst contains Pt, C, V, and O elements.

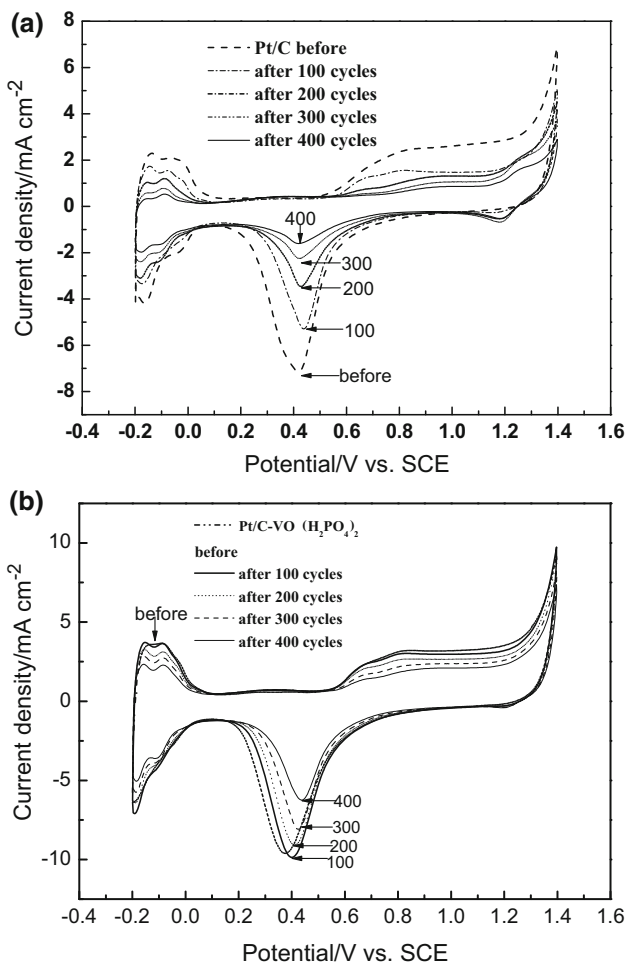


Fig. 6 CV curves of GC with **a** Pt/C and **b** Pt/C–VO(H₂PO₄)₂ before and after the durability test

Table 1 ESA of the Pt/C catalyst and Pt/C–VO(H₂PO₄)₂ catalyst

Cycle number	ESA (m ² g ⁻¹)	
	Before	After 800
Pt/C catalyst	41.86	4.85
Pt/C–VO(H ₂ PO ₄) ₂ catalyst	66.94	34.63

3.2 Electrochemical performance of the catalyst

Figure 4 exhibits the oxidation and reduction peaks that correspond to those of a V_[VI]/V_[V] couple. These peaks were observed at approximately 1.4 and 0.7 V (vs. SCE). Figure 5 compares the CV measurements of different ratio of VO(H₂PO₄)₂ doping in Pt/C catalyst. The group with 6 % doping shows the best electrochemical activity was best of all, and thus the ideal VO(H₂PO₄)₂ ratio (6 %) was determined. The oxidation and reduction peaks of V_[VI]/V_[V] cannot be distinguished, possibly because of the oxygen

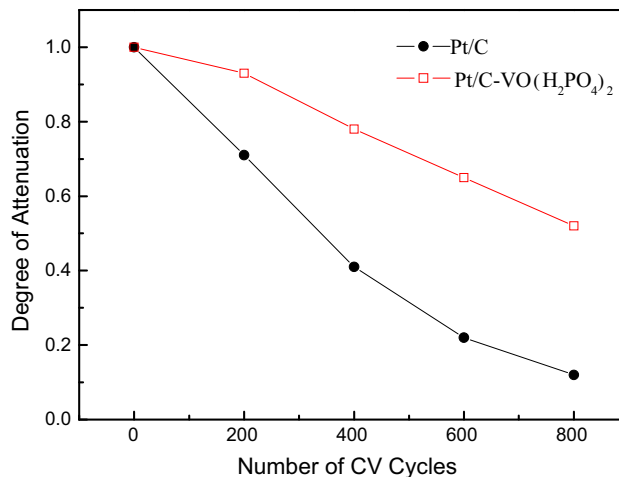


Fig. 7 Remaining ESA after the CV cycles of Pt

adsorption and the V_[VI]/V_[V] oxidation at the same potential.

3.3 Durability test of a three-electrode cell

Electrochemical analyses were performed in situ to ignore GC electrode degradation before and after the durability test. Figure 6 shows the comparison of the CV measurements of Pt/C catalyst and Pt/C–VO(H₂PO₄)₂ catalyst before and after the durability test. The CV findings were considered in determining the ESA with the electrochemical analyzer system Autolab PGSTAT302 N potentiostat. The scanning range was limited at –0.2 to 1.4 V (vs. SCE), and the scanning rate was 50 mV s⁻¹. CV curves were recorded to calculate the ESA of Pt in the catalysts using Eq. (1).

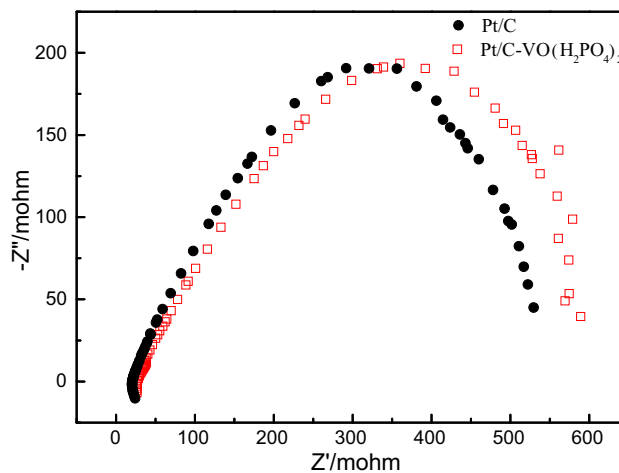
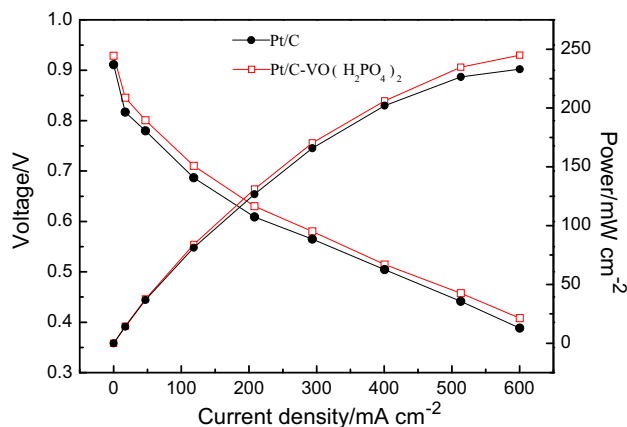


Fig. 8 Electrochemical impedance spectra before and after the durability test on the MEAs with Pt/C–VO(H₂PO₄)₂ and Pt/C catalyst

Table 2 Fitting data of the Nyquist plots on the basis of EIS measurement

	R_s (m Ω)	R_p (m Ω)
Pt/C catalyst	20.67	508.88
Pt/C–VO(H ₂ PO ₄) ₂ catalyst	26.91	553.21

**Fig. 9** Polarization curves of a single cell with Pt/C–VO(H₂PO₄)₂ and Pt/C catalyst

The calculated ESA of the Pt in the Pt/C catalyst and the Pt/C–VO(H₂PO₄)₂ catalyst is presented in Table 1. Prior to the durability test, the initial ESA value of the Pt in Pt/C–VO(H₂PO₄)₂ is 66.94 m² g^{−1}. This value is greater than that of the Pt in Pt/C (41.86 m² g^{−1}). Furthermore, the ESA value of the Pt in Pt/C is reduced to 4.85 m² g^{−1} after 800 CV test cycles; thus, the remaining ESA of the Pt in Pt/C is approximately 12 %. By contrast, the ESA value of the Pt in Pt/C–VO(H₂PO₄)₂ is significantly greater than that of the Pt in Pt/C at 34.63 m² g^{−1} under the same condition. Therefore, the remaining ESA of the Pt in Pt/C–VO(H₂PO₄)₂ is roughly 52 %, as is presented in Fig. 7. These results indicate that the Pt/C–VO(H₂PO₄)₂ catalyst is more durable than the Pt/C catalyst. This improved durability can be ascribed to the fact that when the fuel cell operates at high potential, VO²⁺ is oxidized to VO₂⁺. The preferential oxidation protects the carbon carriers against oxidation. When the fuel cell returns to normal working potential, the VO₂⁺ is restored to VO²⁺. VO²⁺ is a reserve for the protection of carbon support at the subsequent instance of high potential. Moreover, the oxide between Pt particles coats the surface of the carbon carriers and limits the aggregation and loss of Pt. These two functions enhance the durability of fuel cell electrodes.

3.4 Single-cell test

Changes in the resistance of the fabricated catalysts at 0.8 V were measured with EIS. The spectra are shown in Fig. 8.

The Nyquist plot of the electrodes consisted of a large semicircle at the high frequency region and a rising line at the low-frequency region. The experimental data are shown in Table 2, in which R_s represents the ohmic resistance of the electrolyte and working electrode, and R_p represents the charge transfer resistance at the interface between the electrode and electrolyte. The calculated parameters of the equivalent circuit are listed in Table 2 and indicate that the values of R_s are almost equivalent in the Pt/C–VO(H₂PO₄)₂ and Pt/C catalyst. This finding suggests that the two different electrodes were properly measured under the same conditions. The presence of a semicircle implies that impedance can be ascribed to R_p at the electrode–electrolyte interface. The fits of R_p for the Pt/C–VO(H₂PO₄)₂ and Pt/C catalyst are almost equivalent, thus indicating that the addition of VO(H₂PO₄)₂ did not decelerate the charge transfer process. This result is consistent with the CV result. The electrode performance is not optimized; therefore, the cell performance shown in Fig. 9 differs from reported in the references. Nonetheless, both EIS and CV results show that the addition of VO(H₂PO₄)₂ did not affect the electrochemical activity of the Pt/C catalyst negatively.

4 Conclusions

Pt/C–VO(H₂PO₄)₂ catalyst was synthesized through a hydrothermal method. The addition of VO(H₂PO₄)₂ did not have a negative effect on the homogenization and the electrochemical activity of the Pt/C catalyst. Pt/C–VO(H₂PO₄)₂ also enhanced the durability of PEMFCs as a catalyst. In addition, physical and electrochemical techniques were used to investigate the structure, performance, and durability of the catalysts. The results obtained with regard to ESA loss, particle size distribution, polarization behavior, and electrochemical impedance spectra indicated that the Pt/C–VO(H₂PO₄)₂ catalyst was more durable than the Pt/C catalyst.

Acknowledgments This research was funded by the National Basic Research Program of China (973 Program, Grant No. 2012CB215500) and the National Natural Science Foundation of China (No. 21406024).

References

1. Sato Y, Wang Z, Takagi Y (2006) Effect of anode catalyst support on MEA degradation caused by hydrogen-starved operation of a PEFC. *ECS Trans* 3:827–833
2. Dingreville R, Qu J, Cherkaoui M (2005) Surface free energy and its effect on the elastic behavior of nano-sized particles, wires and films. *J Mech Phys Solids* 53:1827–1854
3. Chung CG, Kim L, Sung YW, Lee J, Chung JS (2009) Degradation mechanism of electrocatalyst during long-term operation of PEMFC. *Int J Hydrogen Energy* 34:8974–8981

4. Ferreira PJ, laO' GJ, Shao-Horn Y (2005) Instability of Pt/C electrocatalysts in proton exchange membrane fuel cells. *J Electrochem Soc* 152:A2256–A2271
5. Zhang J, Sasaki K, Sutter E, Adzic RR (2007) Stabilization of platinum oxygen-reduction electrocatalysts using gold clusters. *Science* 315:220–222
6. Mayrhofer KJJ, Meier JC, Ashton SJ et al (2008) Fuel cell catalyst degradation on the nanoscale. *Electrochem Commun* 10:1144–1147
7. Luo Z, Li D, Tang H, Pan M, Ruan R (2006) Degradation behavior of membrane-electrode-assembly materials I 10-cell PEMFC stack. *Int J Hydrogen Energy* 31:1831–1837
8. Mitsushima S, Sawahara S, Ota K, Kamiya NJ (2007) Consumption rate of Pt under potential cycling. *Electrochem Soc* 154:B153–158
9. Wang X, Kumar R, Myers DJ (2006) Effect of voltage on platinum dissolution relevance to polymer electrolyte fuel cells. *Electrochem Solid State Lett* 9:A225–A227
10. Cheng X, Shi Z, Glass N (2007) A review of PEM hydrogen fuel cell contamination: impacts, mechanisms, and mitigation. *J Power Sources* 165:739–756
11. Garzon FH, Rockward T, Urdampilleta IG, Brosha EL, Uribe FA (2006) The impact of hydrogen fuel contaminations on long-term PEMFC performance. *ECS Trans* 3:695–703
12. Franck-Lacaze L, Bonnet C, Besse S, Lopicque F (2009) Effects of ozone on the performance of a polymer electrolyte membrane fuel cell. *Fuel Cells* 9:562–569
13. Mukerjee S, Srinivasan S (1993) Enhanced electrocatalysis of oxygen reduction reaction on platinum alloys in proton-exchange membrane fuel cells. *J Electroanal Chem* 357:201–224
14. Franco AA, Passot S, Fugier P et al (2009) Pt_xCo_y catalyst degradation in PEFC environments: mechanistic insights I. Multiscale modeling. *J Electrochem Soc* 156:B410–B424
15. Antolini E, Salgado JRC, Gonzalez ER (2006) The stability of Pt–M alloy catalysts and its effect on the activity in low temperature fuel cells, a literature review and text on a Pt–Co catalyst. *J Power Source* 160:957–968
16. Nørskov JK, Bligaard T, Hvolbæk B, Abild-Pedersen F, Chorkendorff I, Christensen CH (2008) The nature of the active site in heterogeneous metal catalysis. *Chem Soc Rev* 37:2163–2171
17. Liu Z, Tian ZQ, Jiang SP (2006) Synthesis and characterization of Nafion-stabilized Pt nanoparticles for polymer electrolyte fuel. *Electrochim Acta* 52:1213–1220